energy&fuels

Article

pubs.acs.org/EF

Controlling Nonpolar Colloidal Asphaltene Aggregation by Electrostatic Repulsion

Sara M. Hashmi* and Abbas Firoozabadi*

Department of Chemical and Environmental Engineering, Yale University, New Haven, Connecticut 06510, United States

Supporting Information

ABSTRACT: While aromatic chemicals are applied to petroleum oil systems to thermodynamically prevent asphaltene precipitation, amphiphilic dispersants can truncate the precipitation process and create stable suspensions of asphaltene colloids in the submicrometer size range. Bulk sedimentation and dynamic light scattering have shown that stabilizing dispersants inhibit colloidal asphaltene aggregation at approximately the same concentration as is needed to effectively slow bulk sedimentation. At the same time, these same types of dispersants can alter the electrostatic properties of colloidal asphaltenes in nonpolar suspensions. While electrostatic stabilization has been linked to aggregation dynamics in several types of colloidal systems, both aqueous and nonpolar, the complete linkage between electrostatic interactions and aggregation inhibition has yet to be shown in colloidal asphaltene suspensions. In this work, we present dynamic light scattering and electrophoresis measurements in colloidal asphaltene suspensions, using three different petroleum fluids and a dispersant which truncates asphaltene precipitation and colloidal aggregation by enabling uniform electrostatic charging at the colloidal asphaltene surface.

INTRODUCTION

Asphaltenes, the largest and most aromatic component of petroleum fluids, can undergo a liquid−liquid phase separation which leads to complete precipitation, often clogging wellbores and pipelines. Thermodynamic inhibition and cleaning methods rely on complete asphaltene solubilization or redissolution of the asphaltene precipitate. Stabilizing dispersants, on the other hand, can operate in the regime of colloidal asphaltene suspensions.[1−3] The nonpolar nature of petroleum systems requires special care in understanding and controlling the factors which can stabilize colloidal asphaltenes. Dispersant type plays an important role in determining how such stabilization occurs in nonpolar suspensions, which have been investigated on several fronts in colloidal science. Whereas ionic dispersants can electrostatically stabilize colloids in nonpolar suspension through the introduction of inverse micelles, nonionic dispersants can even stabilize colloidal suspensions at concentrations below their critical micelle concentration (cmc).[4−6]

Asphaltenes, defined as being soluble in aromatics such as toluene, and insoluble in medium-chain alkanes like heptane, have molecular-scale sizes in the nanometer range.[7−10] The molecular size characteristics of asphaltenes are best investigated in equilibrium solutions of isolated aspahltenes fully dissolved in toluene, through techniques like neutron and X-ray scattering. Due to their propensity toward $\pi-\pi$ interactions, asphaltene molecules associate; even when dissolved in toluene they can exhibit molecular sizes up to 25 nm or even larger with an increase in temperature.[11,12] Fractionation by ultracentrifuge followed by X-ray scattering reveals associated asphaltene molecular sizes anywhere between 3 and 25 nm.[11] Composition is of utmost importance in considering the nature of asphaltenes in a mixture. Adding heptane below the onset of asphaltene precipitation leads to an increase in asphaltene molecular size, while still maintaining molecular equilibrium of the asphaltenes in Heptol. For instance one study reports an increase from 7 to 20 nm upon the addition of 45% heptane.[8] An excess of heptane, however, leads to complete precipitation and separation. In this case, asphaltenes are no longer in equilibrium with the solution; their association cascades into the colloidal scale, and dynamics must be considered. Asphaltenes undergoing precipitation in a slight excess of heptane exhibit colloidal aggregation over a time scale of hours, which can be greatly accelerated by the addition of even more heptane.[13,14] Without any toluene to provide thermodynamic stabilization, the colloidal growth and aggregation of asphaltenes in a great excess of heptane can lead to complete separation within minutes.[2]

At the same time, evidence of stabilizing repulsive electrostatic interactions has recently been reported in nonpolar colloidal asphaltenes suspensions in heptane with the addition of dispersants.[15] The effect of three different dispersants was measured: two proprietary nonionic dispersants and one well-known anionic dispersant. This previous work was performed on suspensions of a model oil consisting of isolated asphaltenes dissolved in toluene and reprecipitated in heptane. The two nonionic dispersants effectively truncated colloidal asphaltene growth and increased electrophoretic mobility, all at concentrations less than their critical micelle concentrations in heptane. The nonionic dispersants adsorbed to negative charges on the asphaltene colloids, thereby promoting positively charged colloids. By contrast, while the ionic dispersant induced some charge in the suspension above its cmc, it did not not effectively truncate colloidal asphaltene growth. Micelles of the ionic dispersant induced only weakly negative charges on the asphaltene colloids. However, while the

Received: April 3, 2012
Revised: May 31, 2012
Published: June 4, 2012

   dx.doi.org/10.1021/ef3005702 | *Energy Fuels* 2012, 26, 4438−4444

presence of electrostatics was observed in the model asphaltene suspensions, it was not directly linked to the prevention colloidal asphaltene aggregation. At the same time, steric stabilization has also been implicated in the asphaltene literature as a necessity for asphaltene stabilization.[16,17] Furthermore, measurements investigating the importance of electrostatic stabilization were not undertaken in real asphaltene systems.

In this study, we use real asphaltene suspensions from three different petroleum fluids, created by mixing each fluid with heptane. We investigate the effect of a previously studied nonionic dispersant in stabilizing colloidal asphaltene suspensions. We use light scattering methods to measure particle size and growth dynamics along with surface charge characteristics. Theories of colloidal stabilization in the literature link aggregation rates to interparticle interactions, which are in turn related to particle characteristics such as size and electrophoretic mobility.[18−20] By measuring both aggregation dynamics and particle characteristics on the same set of suspension compositions, we obtain two independent measures of stability, thereby confirming the connection between electrostatics and stability against aggregation. Furthermore, we observe similar trends in suspensions made from each of the three petroleum fluids we investigate, suggesting the possibility of a unified treatment of colloidal asphaltene suspension stability.

MATERIALS AND METHODS

Materials. We obtain three petroleum fluids, called SB, QAB, and CV. We characterize their asphaltene content by filtration. We precipitate asphaltenes by adding heptane, and define the heptane ratio χ, with units of milliliters per gram, indicating the number of millileters of heptane (Fischer) combined with 1 g petroleum fluid. The asphaltene content of the three fluids is measured as reported previously, by mixing the petroleum fluid with heptane at χ = 40 mL/g.[2] The mixtures are soniccated for 1 min and filtered through 0.2 μm pore-size cellulose nitrate membrane filters (Whatman). The filtrate is collected, dried, and weighed to give a fraction of asphaltenes in the oil, f. The density ρ_a of the asphaltenes is measured by preparing a mixture with 0.04 g asphaltenes with 15 mL toluene and measuring the density of the mixture using a densitometer (Anton Paar). On the basis of 10−12 measurements, we measure the asphaltene density ρ_a in grams per milliliter, obtaining measurements within error bars of other values presented in the literature.[3,21,22] We also measure the density of the petroleum fluids themselves, ρ, in grams per milliliter. The characteristics of the three fluids are compiled in Table 1.

We obtain a proprietary nonionic dispersant of the polyolefin alkeneamine class with molecular weight ∼2000, which we call BA (Lubrizol Corporation). We use the dispersant as received and prepare stock solutions in heptane at various concentrations c in parts per million by weight. Light scattering and conductivity measurements indicate a critical micelle concentration of c_c = 10 ppm in heptane.[15]

Table 1. Material Properties: Asphaltene Fraction f, Asphaltene Density ρ_a, and Fluid Density ρ for the SB, QAB, and CV Fluids

petroleum fluid	f	ρ_a	ρ
SB	0.0069	1.1 ± 0.090	0.848
QAB	0.0125	1.1 ± 0.001	0.871
CV	0.0803	1.2 ± 0.005	0.895

Dynamic Light Scattering. We assess the effect of BA on the asphaltene colloids in heptane suspensions using phase-analysis light scattering to measure the electrophoretic mobility μ (ZetaPALS, Brookhaven Instruments). To characterize the size a of the particles, we use dynamic light scattering at wavelength λ = 658 nm and wave vector q = 0.01872 nm^{-1} (ZetaPALS, Brookhaven Instruments).

At c = 0 ppm, we prepare samples over a range of asphaltene volume fraction ϕ, which is related to the heptane ratio: $\phi = f/(\rho_a\chi)$. Because asphaltenes absorb light, we must use sufficiently dilute suspension preparations for effective measurement with the light scattering techniques. To determine appropriate compositions with a sufficient scattered light signal for further investigation, we monitor the scattered light intensity I as a function of ϕ at c = 0, with ϕ between 6×10^{-5} and 1×10^{-3}. Due to the different asphaltene contents f of the three petroleum fluids, these ranges correspond to χ from 5 to 300 mL/g for SB, 25 to 1000 mL/g for QAB, and 100 to 6000 mL/g for CV.

To assess both electrophoretic mobility μ and particle size a as a function of c, we prepare suspensions with a total volume of 3 mL heptane, at $\phi \sim 2 \times 10^{-4}$ using SB and $\phi \sim 1 \times 10^{-4}$ using QAB and CV. This corresponds to fixed values of χ = 30, 100, and 600 mL/g, for SB, QAB, and CV respectively. To measure particle size a and aggregation rates at low BA concentrations, we collect measurements at 30 s intervals for up to 90 min, depending on the time of aggregation in each sample. In stable suspensions which do not aggregate further, we collect 30 s measurements for at least 10−20 min. Assessment several hours later confirms stability against aggregation.

All measurements are carried out at room temperature and pressure.

RESULTS AND DISCUSSION

Colloidal Aggregation at c = 0 ppm. Colloidal asphaltene instability is linked to fast aggregation and occurs at an intermediate stage of asphaltene precipitation. Understanding the parameters governing aggregation dynamics can help to delay eventual full separation of asphaltenes. Certain signatures in bulk sedimentation in colloidal asphaltene suspensions also occur as a result of aggregation, as discussed further in the Supporting Information.[2,3,23]

Because asphaltenes absorb visible light, we first establish the proper range of compositions to investigate with light scattering, as discussed in the Supporting Information. Increasing the petroleum fluid content in suspension reduces both the scattered light intensity and the data quality to a point where meaningful interpretation of particle size is impossible. To avoid this region of composition, we choose to investigate only those suspensions scattering the maximum intensity of light, corresponding to χ = 30, 100, and 600 mL/g for suspensions of SB, QAB, and CV, respectively. For SB and QAB, this composition ranges to a maximum $\phi \sim 10^{-4}$, while for CV, the maximum allowed $\phi \sim 2 \times 10^{-4}$.

At c = 0 ppm, asphaltene colloids grow to a few micrometers in size before aggregating to a much larger scale, regardless of the type of petroleum fluid used. At early times, the particle size a is roughly constant with t. An average of this initial plateau gives a measurement of a_0 the preaggregate particle size. At

dx.doi.org/10.1021/ef3005702 | Energy Fuels 2012, 26, 4438−4444

some time, denoted as $t_{1/2}$, the size abruptly increases from a_0, indicating the aggregation of isolated asphaltene colloids to a much larger size scale. As more heptane is added to the system, the time of the abrupt aggregation, $t_{1/2}$, becomes delayed. We show an example of this aggregation in Figure 1a, for suspensions of QAB asphaltenes in heptane over a range of ϕ from 5.7 to 9.1 × 10^{-5}.

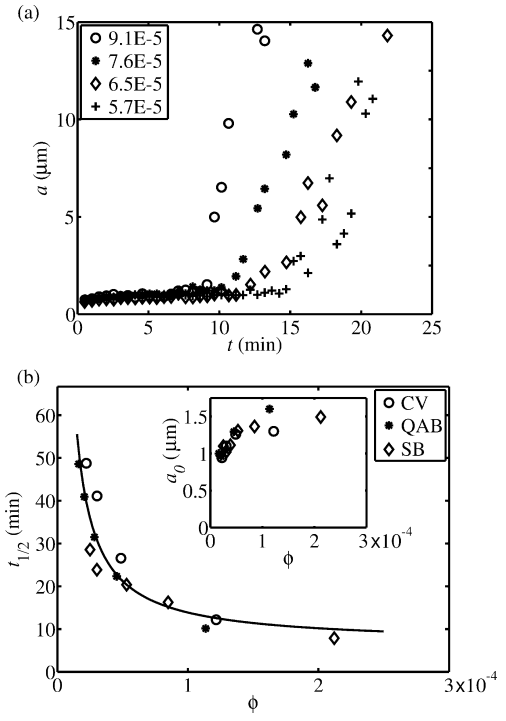

Figure 1. Aggregation with dilution: (a) particle size a as a function of time for suspensions of petroleum fluid QAB with colloidal asphaltene volume fraction ϕ as listed in the legend; (b) time until aggregation $t_{1/2}$ as a function of ϕ.

The delay in aggregation time can be explained by appealing to the aggregation dynamics framework developed by Smoluchowski and, later, Fuchs to describe both rapid and slow aggregation.[18,19] Pairwise interactions lead to collisions between particles, and so the aggregation rate depends linearly on the particle volume fraction ϕ. The aggregation time $t_{1/2}$ increases with particle volume but decreases with particle volume fraction:

$$t_{1/2} = \frac{\pi\eta\rho_a {a_0}^3}{\phi\rho_{C7}k_BT}W \quad (1)$$

where η and ρ_{C7} are the solution viscosity and density, a_0 is the preaggregate colloidal asphaltene size, ρ_a is the asphaltene density, k_B is the Boltzmann factor, and T is temperature.[20] The factor W is called the stability ratio and is given by

$$W = 2a_0 \int e^{U(r)/k_BT} \frac{dr}{r^2} \quad (2)$$

where $U(r)$ is the interaction potential between particles with a separation distance r.[24] In this way, measurements of the aggregation time can provide a measure of W and, therefore, inform us about the interparticle interactions in suspension. Fast aggregation times indicate attractive systems: $U(r) < 0$, hence $W < 1$. With repulsive interparticle interactions, $U(r) > 0$, $W > 1$, and aggregation can be either slow or nonexistent.

Measurements of $t_{1/2}$ can be used to assess W in the colloidal asphaltene systems without dispersant. We vary ϕ by a factor of 6 for each of the three types of suspensions, giving an overall range of $1 \times 10^{-5} < \phi < 2 \times 10^{-4}$. Over this range of ϕ, aggregation times decrease with ϕ, from 50 min to less than 8 at the largest ϕ. For all three types of suspensions, $t_{1/2}$ is well fit by $t_{1/2} = k/\phi$, where the fit constant $k = 0.0436$ gives $R^2 = 0.86$. The dependence of $t_{1/2}$ on ϕ is shown in Figure 1b, where the solid line indicates a fit to the data.

The results indicate that an increasing amount of heptane in suspension slows aggregation simply by reducing the volume fraction of asphaltene particles and therefore the probability of collisions between them. While "dilution slows aggregation" is a general rule of thumb in colloidal systems, this result is remarkable in colloidal asphaltene suspensions. Petroleum fluids are multicomponent mixtures, and asphaltenes have a broad range of characteristics which vary from one source fluid to another. Many factors affect the thermodynamics of asphaltene precipitation, such as asphaltene content of the petroleum, metal content in the asphaltenes, and the amount of resins and other nonasphaltic materials in the source petroleum fluid.[25] The three types of suspensions under investigation in the present study come from three different source petroleum fluids, each with unique properties as shown in Table 1. Despite their differences, aggregation of the asphaltene colloids in heptane, without dispersant, is governed simply by ϕ in this dilution range.

To estimate W from the fit of $t_{1/2} = k/\phi$ in Figure 1b, we need the preaggregate particle size a_0. For all three suspension types, a_0 increases by 30% over the range of ϕ investigated, as seen in the inset to Figure 1b. At $\phi = 2 \times 10^{-5}$, a_0 = 1.1, 1.0, and 0.9 μm for the SB, QAB, and CV suspensions, respectively. These values increase to a_0 = 1.5, 1.6, and 1.3 μm, respectively, for the SB at $\phi = 2 \times 10^{-4}$ and the QAB and CV at $\phi = 1 \times 10^{-4}$. Over the range of ϕ investigated, the average $\langle a_0 \rangle = 1.2 \pm 0.2$ μm for the three suspension types, based on averages of the data shown in the inset to Figure 1b. This value of $\langle a_0 \rangle$ gives an overall $W = 0.06$ at $c = 0$ ppm and correctly reflects the instability in suspensions without dispersant. Using the individual measurements of a_0 and $t_{1/2}$ for each suspension, W varies between 0.04 and 0.16.

Colloidal Aggregation at Fixed ϕ. While dilution slows colloidal asphaltene aggregation simply by decreasing ϕ, the addition of dispersant at fixed ϕ can also slow asphaltene aggregation, albeit through a different mechanism. To investigate the most effectively scattering suspensions, as discussed in the Supporting Information, we choose $\phi = 2 \times 10^{-4}$ for suspensions made with SB and $\phi = 10^{-4}$ for suspensions made with QAB and CV. Without dispersant at these values of ϕ, the asphaltene colloids aggregate within approximately 8−13 min, as seen in Figure 1b. The addition of even less than 1 ppm BA can slow aggregation to 30 min or longer, and 1.5 ppm can inhibit aggregation altogether. An example of this behavior is shown in Figure 2a, for a suspension made with CV at $\phi = 10^{-4}$. BA has this effect on suspensions of all three types, and a summary of $t_{1/2}$ as a function of c is shown in Figure 2b, for $0 < c < 0.7$ ppm. Above $c = 0.7$ ppm, none of the suspensions exhibit aggregation even hours after sample preparation.

An increase of $t_{1/2}$ may indicate an increase in W, as long as a_0 remains constant in the range $0 < c < 0.7$ ppm. At $c = 0$ ppm,

dx.doi.org/10.1021/ef3005702 | Energy Fuels 2012, 26, 4438−4444

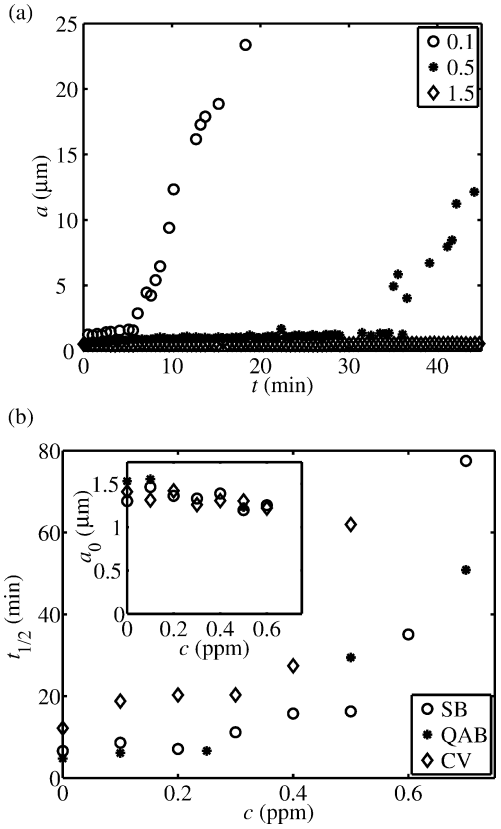

Figure 2. Aggregation with added dispersant: (a) particle size a as a function of time for suspensions of petroleum fluid QAB at colloidal asphaltene volume fraction $\phi = 1 \times 10^{-4}$ and the dispersant concentrations c listed in the legend; (b) time until aggregation $t_{1/2}$ as a function of c.

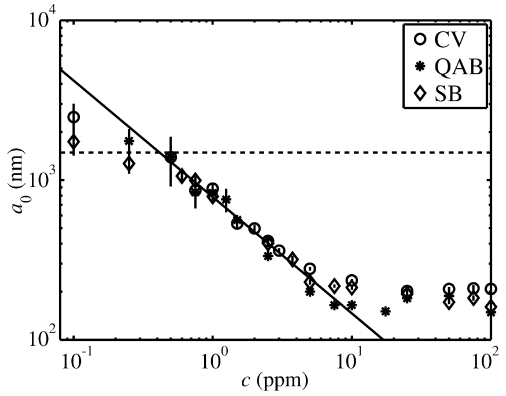

Figure 3. Preaggregate size a_0 as a function of dispersant for each of the three suspension types, all prepared at colloidal asphaltene volume fraction $\phi \sim 10^{-4}$. The solid line is a fit to the data with slope −0.73. The dashed line shows the average value of a_0 for all three suspension types in the absence of dispersant.

a_0 = 1.5, 1.6, and 1.3 μm for the SB, QAB, and CV suspensions, corresponding to the highest ϕ values shown in the inset to Figure 1b. With the increase of c at fixed ϕ, a_0 for asphaltene colloids of all three types decreases by approximately 20%, from 1.5 ± 0.2 at c = 0 ppm to 1.2 ± 0.1 μm at c = 0.7 ppm, based on averages of the data shown in the inset to Figure 2b. The overall average of a_0 across the three types of suspensions over this range of c is $\langle a_0 \rangle$ = 1.4 ± 0.1 μm, a variation of less than 8%. Given the measurements of a_0 and $t_{1/2}$, W increases 2 orders of magnitude between c = 0 and c = 0.7 ppm, from a minimum of 0.02, in the case of the QAB asphaltenes at c = 0 ppm, to nearly 0.8, for the QAB and CV asphaltenes at c = 0.7. Since ϕ is fixed, the increase in W must arise from changes in the interparticle potential.

With the addition of dispersant BA at even larger concentrations than is needed to stop aggregation, the growth of asphaltenes to the colloidal scale becomes truncated. Furthermore, a_0 shrinks by an order of magnitude up to $c \sim$ 7.5 ppm. At this concentration, a_0 plateaus: for SB, the average value of a_0 for c > 7.5 ppm is 190 ± 23 nm; for QAB, it is 165 ± 16 nm; and for CV, it is 215 ± 14 nm. The decrease in a_0 follows a power-law with c: $a_0 \sim c^{-0.73}$, where the power −0.73 has been determined by a fit to the data. This behavior is shown in Figure 3; the error bars are based on 10−40 measurements of 1−3 suspensions at each c. The solid line indicates the power law fit to the data in the range 0.5 < c < 7.5, while the dashed line indicates $\langle a_0 \rangle$ = 1.5 μm at c = 0 ppm for all three types of suspensions, CV, QAB, and SB at fixed $\phi \sim 10^{-4}$. The power law decrease in a_0 with c can be attributed to dispersant adsorption onto the asphaltene colloids during the precipitation process.[15] A simple scaling model showed that the power law exponent is equal to $1/(D_f - 3)$, where D_f is the fractal dimension. For the current results, this model gives D_f = 1.63, a reasonable suggestion compared to other colloidal asphaltene measurements.[15]

Electrophoretic Mobility. In the absence of dispersant, the electrophoretic mobility μ of the asphaltene colloids is very low, requiring the use of a sensitive technique such as phase analysis light scattering (PALS) for effective measurement. Similar to laser Doppler electrophoresis methods, PALS measures $\mu = v/E$ by obtaining the Doppler shift caused by particles moving with velocity v in an electric field E = 2.8 kV/m. The nominal noise floor of the PALS is 10^{-10} m^2/(V s).[20,26] However, the instantaneous velocity of colloidal asphaltenes due to Brownian motion can be interpreted by the PALS technique as a very low electrophoretic mobility corresponding to values as large as 3×10^{-10} m^2/(V s).[27]

At c = 0 ppm, mobility measurements of the asphaltene colloids exhibit a bimodal distribution of μ for all three types of suspensions. Using an effective scattering composition, $\phi \sim 10^{-4}$, we find approximately 45% of the 50 measurements done on each type of suspension yield negative values and 55% yield positive values. For all three types of suspensions, the average value of the negative and positive modes are identical: $\pm 0.055 \times 10^{-8}$m^2/(V s), with a standard deviation of $\pm 0.028 \times 10^{-8}$m^2/(V s), reflecting a 50% spread in the data for each mode. Measurements with magnitude less than 3×10^{-10} m^2/(V s) are not included in the histogram shown in Figure 4. In more dilute suspensions, at $\phi \sim 10^{-5}$, the situation is similar: 35% of the measurements are negative while 65% are positive, with the magnitude of each mode being $\langle \mu_- \rangle = -0.034 \times 10^{-8}$ m^2/(V s) and $\langle \mu_+ \rangle = 0.038 \times 10^{-8}$ m^2/(V s).

While in total the asphaltenes are charge-neutral, the bimodal distribution of μ indicates heterogeneous charging of the asphaltene colloids. Heterogeneous surface charge may explain previously reported electrodeposition results, which indicate that asphaltenes are charged entities that can deposit on either anode or cathode, and sometimes on both anode and cathode from within a single suspension.[28−30] One interpretation of this result is that some particles may carry a small net positive charge, while others carry a small net negative charge, resulting

dx.doi.org/10.1021/ef3005702 | Energy Fuels 2012, 26, 4438−4444

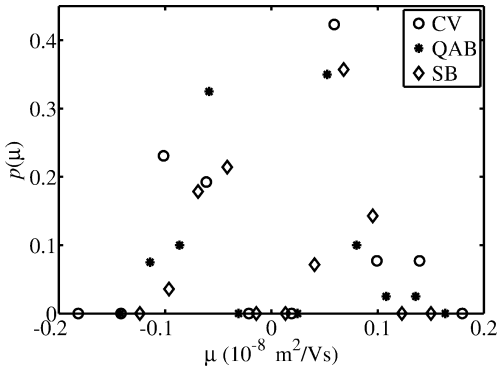

Figure 4. Histogram of electrophoretic mobility measurements $p(\mu)$ at dispersant concentration $c = 0$ for the three types of suspensions, all prepared at colloidal asphaltene volume fraction $\phi \sim 10^{-4}$.

in the bimodal distribution of μ. Asphaltenes are known to contain metallic components, including porphyrinic content, which can influence the stability of asphaltenes in nonpolar systems.[31,32] These same metallic components could contribute to positive charges in the system. Negative charges might arise from the π electron clouds of the polyaromatic hydrocarbon rings that constitute asphaltenes molecules. Zwitterions and acid−base surface groups have also been proposed as a source of charge on asphaltenes.[33,34]

Addition of dispersant BA to the asphaltene suspensions facilitates a net-positive charge on the colloidal asphaltenes. We have linked this phenomena to the adsorption of BA onto negatively charged sites on the asphaltenes: the BA backbone contains conjugated π bonds, which could interact favorably with both heteroatomic lone pairs and aromatic sites on the asphaltenes.[15] To measure this effect we fix the composition of each suspension at $\phi \sim 10^{-4}$. The percentage of negative measurements $\int p(\mu_-)\, d\mu$ decreases with dispersant until the measurements of μ become wholly positive, indicating homogeneous charging on the asphaltene colloids. The decrease in $\int p(\mu_-)\, d\mu$ is shown in Figure 5a. Furthermore, $\langle\mu\rangle$ increases with c up to 10 ppm, where it plateaus at $\langle\mu\rangle \sim 0.17 \times 10^{-8}$ m^2/(V s) for all three types of suspensions. The behavior of $\langle\mu\rangle$ is shown in Figure 5b, for suspensions made with CV, QAB, and SB. This increase in $\langle\mu\rangle$ may help to describe the increasing stability of the system with the addition of dispersants, as seen through the colloidal aggregation measurements. Interestingly, the plateau values of $\langle\mu\rangle$ above c = 10 ppm are comparable to those in other nonpolar colloidal suspensions, like PMMA particles in hexane with Span 85.[6]

The current measurements suggest that both a_0 and μ reach plateaus near 10 ppm of the dispersant BA. BA in heptane has a critical micelle concentration at 10 ppm, and the formation of micelles of BA has been previously shown to halt both the decrease in a_0 and the increase in μ.[15] Ionic dispersants can readily stabilize nonpolar suspensions at concentrations above the critical micelle concentration.[4,35−37] Nonionic dispersants, however, exhibit charge and charge-stabilization of colloids even at concentrations below the cmc.[6,38] In the case of colloidal asphaltene suspensions, a third possibility presents itself: that the charge originates on the asphaltene colloids themselves and does not arise from the dispersant at all. In the limit of very low ionic strength, as in nonpolar colloidal asphaltene suspensions, electrophoretic motion arises directly from the balance between hydrodynamic drag and electrostatic interactions: $\mu = Qe/(6\pi\eta a_0)$, where Q is the total number of

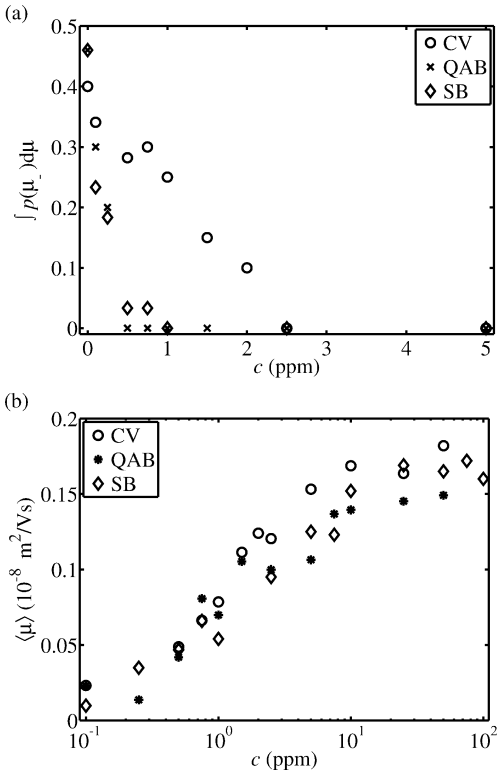

Figure 5. Electrophoretic mobility μ with dispersant: (a) percentage of negative measurements $\int p(\mu_-)\, d\mu$ as a function of added dispersant c; (b) average value $\langle\mu\rangle$ as a function of c. Measurements in each plot are shown for the three types of suspensions all at $\phi \sim 10^{-4}$.

surface charges and e the elementary charge. The decrease in a_0 coupled with the increase in μ over the same range of c suggests constant charge on the colloids regardless of dispersant.[27] The combination of a_0 and μ measurements thus implies an increased surface charge density on the asphaltenes with an increase in dispersant concentration up to the cmc.

Suspension Stability. Control over the factors stabilizing colloidal asphaltene suspensions could have major implications for processing techniques in the petroleum industry. Stability can be measured through aggregation times, as well as through particle characteristics such as size and electrophoretic mobility. While eq 1 applies for suspensions with fixed particle size and interpaticle potentials, we can use the measurements of $t_{1/2}$ and a_0 for the three types of suspensions at fixed ϕ to investigate stability as a function of dispersant concentration. As expected through the behavior of $t_{1/2}$ as seen in Figure 2b, W also increases with c. Using eq 1 to obtain W for each suspension, we find that the aggregation times collected for each of the three suspension types collapse onto a single exponential curve $W(c)$, as seen in Figure 6a. The solid line is a fit to the data: $W = 0.04 \exp(3.8c)$. We have access to W through aggregation measurements only at $c < 0.7$ ppm, at which concentrations the colloidal asphaltenes aggregate. Furthermore, the values of W measurable in aggregating suspensions must be less than 1, indicating instability.

The dependence of W on c suggests an exponentially increasing repulsion between particles in the suspensions with the addition of dispersant. Given the measured increase in μ with c, we express the interparticle potential as a summation of attractive dispersion interactions and bare Coulombic repulsive electrostatic interactions:

dx.doi.org/10.1021/ef3005702 | Energy Fuels 2012, 26, 4438−4444

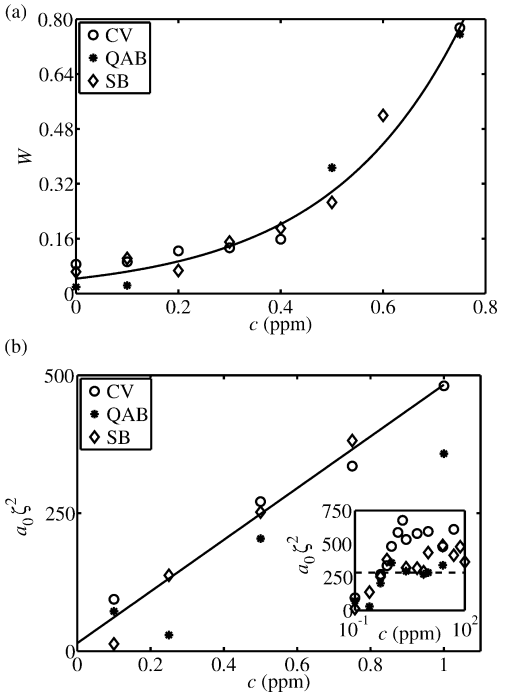

Figure 6. Stability with dispersant: (a) stability ratio W as a function of dispersant, obtained from measurements of aggregation time $t_{1/2}$ and eq 1—the solid line is an exponential fit to the data; (b) measured values of $a_0\zeta^2$ as a function of dispersant concentration c up to 1 ppm (main plot) and up to 100 ppm (inset). The solid line is a linear fit to the data. The dashed line in the inset shows $a_0\zeta^2 = 280$. All three plots show results for the three suspensions prepared at colloidal asphaltene volume fraction $\phi \sim 10^{-4}$.

$$U(r) = -\frac{a_0 A_{121}}{12r} + \frac{4\pi D\varepsilon_0 {a_0}^2 {\Phi_0}^2}{r + 2a_0} \quad (3)$$

where A_{121} is the Hamaker constant, D the dielectric constant of the liquid, ε_0 the permittivity of free space, and Φ_0 the surface potential.[20] With this assumption, the stability ratio becomes

$$W \simeq \left(\frac{A_{121}{k_B}^2 T^2}{3072 D^3 {\varepsilon_0}^3 {a_0}^3 {\Phi_0}^6}\right)^{1/4} \exp\left(\frac{2\pi D\varepsilon_0 a_0 {\Phi_0}^2}{k_B T}\right) \quad (4)$$

The argument of the exponent depends only on the electrostatic repulsion, while the constant has contributions from both attractive van der Waals forces and repulsive electrostatics.[24]

The observed exponential increase in W as a function of c matches the expected form of W for bare Coulomb electrostatic repulsion as seen in eq 4. While eq 4 does not have an explicit dependence on c, both a_0 and μ change with added dispersant. Using $W = 0.04\exp(3.8c)$, the fit based on measurements of t_{agg} shown in Figure 6a, along with the constants in eq 4, we obtain $a_0{\Phi_0}^2 = 150c$. The surface potential Φ_0 can be approximated through the zeta potential ζ. Given the long screening lengths in nonpolar asphaltene suspensions, Huckel theory gives $\zeta = 3\mu\eta/(2D\varepsilon_0)$.[15] Therefore, we can assess stability even in suspensions which do not aggregate, through measurements of a_0 and ζ.

As expected by Coulombic repulsion and the exponential increase of W at low c, the measurements of a_0 and ζ give a linear increase in $a_0\zeta^2$ with c, as shown in Figure 6b. The solid line is a fit to the data: $a_0\zeta^2 \sim 494c$. The slope of $a_0\zeta^2(c)$ predicted through the aggregation measurements is a factor of 3 smaller than the slope obtained through direct mesurements of a_0 and ζ. Carrying the measured behavior of $a_0\zeta^2(c)$ through eq 4 suggests $W = 0.06\exp(11.9c)$, a faster exponential increase in stability than observed through the aggregation measurements. In other words, asphaltene colloids aggregate more readily at $c < 0.7$ ppm than the measurements of a_0 and ζ would suggest. The behavior of $\mu(c)$ may explain this faster-than-expected aggregation: while $\langle\mu\rangle$ increases with c, as in Figure 5b, we also observe that negative charges persist at low c, as seen in Figure 5b. Heterogeneous surface charging at low c could therefore facilitate aggregation. For this reason, estimates of W using t_{agg} are lower than those predicted from a_0 and ζ.

Stable dispersions are often defined as having $W > 10^5$.[24] Given eq 4, and using the literature value of $A_{121} = 1.1 \times 10^{-21}$ J, that criterion becomes $a_0\zeta^2 > 280$.[39] In general, colloidal suspensions of larger particles are more stable than those with smaller particles because U increases with a, as seen in eq 3. In the case of colloidal asphaltenes, however, the opposite seems to be true: suspensions stabilized by dispersant are those with smaller particles, not larger. This can be seen in the measurement of $a_0\zeta^2$ shown in Figure 6b: $a_0\zeta^2$ climbs above 280 near $c = 0.6$ ppm. The inset to Figure 6b shows $a_0\zeta^2$ over a wider concentration range: beyond $c = 1$ ppm as shown in the main figure, $a_0\zeta^2$ remains above 280. Suspensions become and remain stable at $c > 1$ ppm. Between $c = 1$ and 10 ppm, a_0 decreases, as shown in Figure 3. In this same concentration range, μ and therefore ζ increase, as seen in Figure 5b. The increase in ζ trumps the decrease in a_0, and for colloidal asphaltenes, smaller particles lead to more stable suspensions. Furthermore, while the colloidal asphaltene characteristics have the same general trends across the three different suspensions types, the composite behavior of $a_0\zeta^2$ indicates that suspensions made from CV have greater stability than the other two. The different stabilities of the three types of suspensions at $c > 1$ ppm may arise from molecular differences between the asphaltenes, such as their characteristic metal content.

CONCLUSIONS

By simultaneously measuring colloidal particle characteristics and aggregation dynamics in real asphaltene suspensions, our results provide a strong link between stability and electrostatics. While steric stabilization has been implicated throughout the asphaltene literature, here we show that sterics may not be necessary: electrostatic repulsion is sufficient to stabilize asphaltene colloids against aggregation.

The electrostatic stabilization provided by dispersant BA accounts for the inhibition of colloidal asphaltene aggregation. Measurements of aggregation time suggest that, in the absence of an effective amount of dispersant, the asphaltene colloids aggregate more readily than expected based on electrophoretic mobility measurements. The bimodal distribution of surface charge on the asphaltene colloids could account for the lessened stability at low c. The ability of asphaltenes to $\pi-\pi$ bond may also play a role. The effective adsorption of dispersant at $c > 1$ ppm prevents further aggregation of the asphaltene colloids. Up until the cmc is reached, the dispersant increases the surface charge density on the colloids as their growth stops at increasingly smaller sizes. Given this understanding, control over colloidal asphaltene suspension stability may be obtained simply from knowledge of the dispersant adsorption characteristics. Combined with the observation that

dx.doi.org/10.1021/ef3005702 | Energy Fuels 2012, 26, 4438−4444

ϕ alone accounts for aggregation instabilities in the absence of dispersant, the present results bode well for the possibility of a unified treatment of dispersant-stabilized colloidal asphaltene suspensions.

■ ASSOCIATED CONTENT

Supporting Information

Supporting DLS screening measurements identify the proper range of suspension compositions appropriate for the light scattering technique, using all three petroleum fluids. Bulk sedimentation dynamics measurements of the asphaltene suspensions are discussed. Representative results are shown for QAB suspensions, namely sedimentation dynamics at $c = 0$ ppm over a range of ϕ, and at fixed ϕ and over a range of c. This information is available free of charge via the Internet at http://pubs.acs.org/.

■ AUTHOR INFORMATION

Corresponding Author

*E-mail: sara.hashmi@yale.edu (S.M.H.); abbas.firoozabadi@yale.edu (A.F.).

Notes

The authors declare no competing financial interest.

■ ACKNOWLEDGMENTS

We gratefully acknowledge the support of RERI member institutions, and the assistance of Kathy Xinyi Zhong and Salvatore DeLucia in the dynamic light scattering measurements.

■ REFERENCES

(1) Kraiwattanawong, K.; Fogler, H. S.; Gharfeh, S. G.; Singh, P.; Thomason, W. H.; Chavadej, S. *Energy Fuels* **2009**, *23*, 1575−1582.
(2) Hashmi, S. M.; Quintiliano, L. A.; Firoozabadi, A. *Langmuir* **2010**, *26*, 8021.
(3) Hashmi, S. M.; Firoozabadi, A. *J. Phys. Chem. B* **2010**, *114*, 15780−15788.
(4) Hsu, M. F.; Dufresne, E. R.; Weitz, D. A. *Langmuir* **2005**, *21*, 4881−4887.
(5) Sainis, S. K.; Germain, V.; Mejean, C. O.; Dufresne, E. R. *Langmuir* **2008**, *24*, 1160−1164.
(6) Espinosa, C. E.; Guo, Q.; Singh, V.; Behrens, S. H. *Langmuir* **2010**, *26*, 16941.
(7) Gawrys, K. L.; Kilpatrick, P. K. *J. Colloid Interface Sci.* **2005**, *288*, 325−334.
(8) Fenistein, D.; Barre, L.; Broseta, D.; Espinat, D.; Livet, A.; Roux, J.-N.; Scarsella, M. *Langmuir* **1998**, *14*, 1013−1020.
(9) Barre, L.; Simon, S.; Palermo, T. *Langmuir* **2008**, *24*, 3709−3717.
(10) Roux, J.-N.; Broseta, D.; Deme, B. *Langmuir* **2001**, *17*, 5085−5092.
(11) Fenistein, D.; Barre, L. *Fuel* **2001**, *80*, 283−287.
(12) Espinat, D.; Fenistein, D.; Barre, L.; Frot, D.; Briolant, Y. *Energy Fuels* **2004**, *18*, 1243−1249.
(13) Anisimov, M. A.; Yudin, I. K.; Nikitin, V.; Nikolaenko, G.; Chernoutsan, A.; Toulhoat, H.; Frot, D.; Briolant, Y. *J. Phys. Chem.* **1995**, *99*, 9576−9580.
(14) Yudin, I. K.; Nikolaenko, G. L.; Gorodetskii, E. E.; Markhashov, E. L.; Agayan, V. A.; Anisimov, M. A.; Sengers, J. V. *Physica A* **1998**, *251*, 235−244.
(15) Hashmi, S. M.; Firoozabadi, A. *Soft Matter* **2011**, *7*, 8384−8391.
(16) Chang, C.-L.; Fogler, H. S. *Langmuir* **1994**, *10*, 1749−1757.
(17) Arteaga-Larios, F.; Cosultchi, A.; Perez, E. *Energy Fuels* **2005**, *19*, 477−484.
(18) van Smoluchowski, M. *Z. Phys. Chem., Stoechiom. Verwandschaftsl* **1917**, *92*, 129−168.
(19) Fuchs, N. *Z. Phys. Chem.* **1934**, *171*, 199−208.
(20) Morrison, I.; Ross, S. *Colloidal Dispersions*; John Wiley and Sons: New York, NY, 2002.
(21) Yen, T. F.; Erdman, G.; Hanson, W. E. *J. Chem. Eng. Data* **1961**, *6*, 443.
(22) Diallo, M. S.; Cagin, T.; Faulon, J. L., III; W., A. G. In *Asphaltenes and Asphalts, 2. Developments in Petroleum Science*; Yen, T. F., Chilingarian, G. V., Eds.; Elsevier Science: New York, 2000; pp 103−127.
(23) Siffert, B.; Kuczinski, J.; Papirer, E. *J. Colloid Interface Sci.* **1990**, *135*, 107.
(24) Morrison, I. D. *Langmuir* **1991**, *7*, 1920−1922.
(25) Mullins, O. C. *Energy Fuels* **2010**, *24*, 2179−2207.
(26) McNeil-Watson, F.; Tscharnuter, W.; Miller, J. *Colloids Surf., A* **1998**, *140*, 53−57.
(27) Hashmi, S. M.; Firoozabadi, A. *Soft Matter* **2012**, *8*, 1878−1883.
(28) Preckshot, G. W.; Delisle, N. G.; Cottrell, C. E.; Katz, D. L. *AIME Trans.* **1943**, *151*, 188−194.
(29) Katz, D. L.; Beu, K. E. *Ind. Eng. Chem.* **1945**, *43*, 1165.
(30) Taylor, S. E. *Fuel* **1998**, *77*, 821−828.
(31) Kaminski, T. J.; Fogler, H. S.; Wolf, N.; Wattana, P.; Mairal, A. *Energy Fuels* **2000**, *14*, 25−30.
(32) Groenzin, H.; Mullins, O. C. *Energy Fuels* **2000**, *14*, 677−684.
(33) Cratin, P. D. *Ind. Eng. Chem.* **1969**, *61*, 35−45.
(34) Speight, J. G. *Oil Gas Sci. Technol.* **2004**, *79*, 479−488.
(35) Sainis, S. K.; Germain, V.; Dufresne, E. R. *Phys. Rev. Lett.* **2007**, *99*, 018303.
(36) Poovarodom, S.; Berg, J. C. *J. Colloid Interface Sci.* **2010**, *346*, 370−377.
(37) Roberts, G. S.; Sanchez, R.; Kemp, R.; Wood, T.; Bartlett, P. *Langmuir* **2008**, *24*, 6530.
(38) Guo, Q.; Singh, V.; Behrens, S. H. *Langmuir* **2010**, *26*, 3203−3207.
(39) Wang, S.; Liu, J.; Zhang, L.; Masliyah, J.; Xu, Z. *Langmuir* **2010**, *26*, 183−190.